Main-chain degradable star polymers comprised of pH-responsive hyperbranched cores and thermoresponsive polyethylene glycol-based coronas

Ulrike Wais,[a,b] Lohitha Rao Chennamaneni,[a] Praveen Thoniyot,[a] Haifei Zhang[b,*] and Alexander W. Jackson[a,*]

[a] Institute of Chemical and Engineering Sciences, Jurong Island, 627833, Singapore.
[b] Department of Chemistry, University of Liverpool, Liverpool L69 7ZD, UK.
* Corresponding authors

Abstract

Core-shell polymeric architectures possessing stimuliresponsive behavior have great potential in triggered release systems, especially biomedical applications. Simultaneously achieving stimuliresponsive behavior and main-chain degradability is an interesting challenge facing modern polymer scientists. We report, the synthesis of star hyperbranched polymers possessing covalently cross-linked pH-responsive cores and linear thermoresponsive PEG-based coronas. Main-chain degradability throughout these structures is achieved via radical ring-opening polymerization of the cyclic ketene acetal 2-methylene-1,3-dioxepane, in combination with reversible-deactivation radical polymerization (RDRP) of methacrylate-based monomers. A two-step reversible addition-fragmentation chain-transfer (RAFT) polymerization is employed, initially facilitating the copolymerization of 2-(diethylamino)ethyl methacrylate and the divinyl cross-linker di(ethylene glycol) dimethacrylate to prepare pH-responsive hyperbranched polymers. Subsequent chain-extension with oligoethylene glycol methacrylate introduces a linear corona. Their ability to uptake and release hydrophobic actives in response to changes in pH is compared to a linear diblock copolymer micellar analogue. The star hyperbranched polymers have been modified post-polymerization by aminolysis to introduce reactive thiol sites, followed by thiol-maleimide click chemistry providing additional peripheral functionality. Hydrogels have also be prepared via disulfide bond formation between multiple star hyperbranched polymers. Finally, the synthetic methodology presented is further improved incorporating main-chain polyesters into both the hyperbranched core and linear corona. We describe the experimental conditions required to successfully prepare diblock and star hyperbranched polymers incorporating 2-methylene-1,3-dioxepane within each block via RAFT polymerization. The schizophrenic pH- and thermoresponsive self-assembly of these materials is investigated and their hydrolytic degradation presented.

Introduction

Reversible-deactivation radical polymerization (RDRP) techniques[1-3] have given scientists access to a wide range of interesting polymeric architectures, including, multi-block, comb, brush, star-shaped and hyperbranched.[4-6] Of these various topologies, hyperbranched[7] polymers are particularly appealing as they can potentially mimic the branched macromolecular systems found in nature. These structures also possess different chemical and physical properties when compared to their linear counterparts, such as, low viscosity, improved solubility, tunable solution behavior and large numbers of functional groups at their chain-end. Their covalently cross-linked nature also imparts a chemical robustness which isn't present in self-assembled polymeric micelles[8] and vesicles.[9] Additionally, covalent cross-linking can provide access to slower rates and can prevent burst release by providing a higher barrier to diffusion. These advantages have resulted in a considerable level of interest in covalently hyperbranched architectures[10-13] for potential application in catalysis,[14] material modification,[15] bioimaging,[16] drug delivery[17] and dispersion/ solubilization.[18]

Hyperbranched polymers have been synthesized by various methods including ring-opening polymerization[19, 20] and step-growth polymerization.[21, 22] Polymerization initiators which possess a vinyl monomer functional group (*i.e.*, an "inimer") are commonly employed to prepare hyperbranched polymers. This methodology is referred to as self-condensing vinyl polymerization (SCVP),[23, 24] more recently several inimers have been prepared to combine reversible-deactivation radical polymerization techniques with SCVP. Click chemistry has been employed[25] to synthesize an acryloyl trithiocarbonate inimer which prepares hyperbranched polymers via a reversible addition-fragmentation chain transfer (RAFT) polymerization-based SCVP approach. Atom transfer radical polymerization (ATRP)[26, 27] and nitroxide-mediated polymerization (NMP)[28] inimers have also been prepared to facilitate the synthesis of hyperbranched polymers via SVCP. While SVCP is one of the most popular routes to hyperbranched polymers the preparation of inimers can be synthetically challenging. A more synthetically straightforward approach to hyperbranched polymers is the application of a cross-linking co-monomer (typically divinyl) which covalently links growing polymer chains.[29] Perrier was the first to report[30] the synthesis of hyperbranched polymers employing RAFT polymerization and a divinyl cross-linker, the same group has also investigated[31] the influence of different reaction parameters on the formation of RAFT generated hyperbranched polymers. Thurecht has employed[32] RAFT polymerization and a divinyl cross-linker to prepare functional hyperbranched polymers for application in florescence and PET bimodal bioimaging. RAFT polymerization has also been utilized[33] by the Whittaker group to prepare biocompatible hyperbranched polymers which incorporate iodine and fluorine for bimodal molecular imaging, the divinyl cross-linker employed in this work contains a disulfide bond which makes these hyperbranched polymers degradable in the presence of reducing agents. The Sumerlin group has prepared[34] thermo- and redox-responsive hyperbranched polymers via the RAFT copolymerization of *N*,*N*'-bis(acryloyl)cystamine and *N*-isopropylacrylamide, these hyperbranched polymers were then chain-extended with *N,N*-dimethylacrylamide to afford star hyperbranched architectures. More recently Sumerlin and Wagener have employed[35] RAFT polymerization to prepare hyperbranched polymers containing active esters which can be modified post-polymerization to introduce other functionalities. To further improve the utility of hyperbranched polymers their precise synthesis, efficient post-polymerization functionalization and the introduction of stimuli-responsiveness are topics of current interest. Another great drive among contemporary polymer scientists is the development of degradable polymeric materials via radical polymerization.[36,39] While main-chain degradability is easily attained through step growth (condensation) and ionic ring-opening polymerization the ability to incorporate diverse functionality, stimuli-responsiveness and prepare complex architectures with these particular polymerization techniques is not as straightforward when compared to modern radical polymerization methods. Additional monomer functionality can directly interfere with both the step-growth

and ionic polymerization mechanisms. Whereas radical polymerizations have always been appealing due to their tolerance of additional monomer functionality (-OH, -COOH, -NR_2) and the presence of water. The enormous appeal of reversible-deactivation radical polymerization methods is the introduction of a 'living nature' into radical polymerizations which easily facilitates the synthesis of multi-block copolymers while simultaneously tolerating to a wide range of functional groups. Main-chain degradability can be achieved via radical polymerization through the application of monomers which are able to undergo radical ring-opening polymerization (rROP).[36] Within this class of monomers cyclic ketene acetals (CKA) are showing great potential in the preparation of main-chain degradable polyesters via rROP.[37, 38] These monomers can be co-polymerized with various vinyl-based monomers, resulting in the random incorporation of ester functionalities along the polymer main-chain.[39] Recently this approach has been combined with RDRP techniques including RAFT polymerization,[40-44] atom transfer radical polymerization (ATRP)[45-47] and nitroxide mediated polymerization (NMP).[48-50] Of course the primary advantage of RDRP techniques it the ability to prepare multi-block copolymers which are able to undergo self-assembly. Several examples of block copolymers which incorporate cyclic ketene acetal monomers within one of their blocks have been reported. These include the chain-extension of various ATRP-based homopolymers of conventional vinyl monomers with the CKA monomer 5,6-benzo-2-methylene-1,3-dioxepane (BMDO),[51] the chain-extension of a various NMP-based CKA containing terpolymers with styrene,[52] the chain-extension of a RAFT-based poly(N-vinylpyrrolidone) macro-initiator with vinyl esters and the CKA monomer 2-methylene-1,3-dioxepane (MDO)[53, 54] and the chain-extension of a RAFT-based MDO copolymer with vinyl acetate[55]. It has also been shown that a di-functional poly(ethylene glycol)-based RAFT macro-initiator can be successful chain-extended with the BMDO and *N*-isopropylacrylamide to afford an ABA triblock copolymer.[56, 57] However, while these recent examples combining modern RDRP techniques with rROP are very promising examples of multi-block copolymers which incorporator a CKA monomer within each block are very limited.[58]

Herein, we report the synthesis of star hyperbranched (SHB) polymers via RAFT polymerization. These architectures could also be described as shell hyperbranched polymers or unimolecular amphiphilic nanoparticles. Initially, 2-(diethylamino)ethyl methacrylate (DEAEMA) and the divinyl cross-linker di(ethylene glycol) dimethacrylate (DEGDMA) are copolymerized before subsequent chain-extension with oligoethylene glycol methacrylate (OEGMA). We study the pH-responsive properties of a series of SHB polymers and observe their self-assembly into larger star hyperbranched micellar structures. The effect of monomer composition on this self-assembly process is then probed. After optimizing the conditions for SHB polymer synthesis we prepare a conventional diblock (DB) polymer analogue and compare the ability of both the SHB and DB polymer to uptake and release a hydrophobic active in response to changes in pH. We observed significantly higher uptake of the hydrophobic active Indomethacin followed by a slower release profile from the SHB polymer architecture when compared to a conventional DB polymer counterpart. Post-polymerization aminolysis is then employed to introduce thiol functional groups at the SHB polymer periphery which can facilitate functionalization through thiol-maleimide click chemistry. The formation of a hydrogel through disulfide bond formation between multiple SHB polymers is briefly outlined. We are of the opinion that these materials possess similar attractive properties of analogous conventional polymeric micelles with the additional benefit of chemical robustness and higher control of release by diffusion imparted through covalent cross-linking. Finally, our initial research into the preparation of these architectures with the incorporation of main-chain polyester degradability via copolymerization with MDO during both RAFT polymerization steps is presented. We highlight the challenges of preparing multi-block polymers with the incorporation of a CKA monomer within each polymer block and outline the synthetic conditions required to achieve this goal. The synthesis of main-chain degradable SHB and DB polymers is achieved and their pH-responsive nature and hydrolytic degradation presented. To the best of our knowledge this is the first example of the incorporation of a CKA monomer within each section of a multi-block polymeric material prepared by RAFT polymerization.

Experimental Section

Materials and Characterization

4-((((2-Carboxyethyl)thio)carbonothioyl)thio)-4-cyanopentanoic acid (BM1433) was purchased from Boron Molecular. 2-Cyano-2-propyl dodecyl trithiocarbonate (CPDT) was purchased from Sigma Aldrich. Oligoethylene glycol methacrylate monomethyl ether (OEGMA, $M_w \approx$ 300 g/mol), 2-(diethylamino)ethyl methacrylate (DEAEMA) and di(ethylene glycol) dimethacrylate (DEGDMA) were purchased from Sigma Aldrich and were passed through a basic alumina column to remove inhibitor prior to use. Azobisisobutyronitrile (AIBN) and azobis(cyanocyclohexane) (ACHN) were purchased from Sigma Aldrich and were used as received. 2-Methylene-1,3-dioxepane (MDO) was prepared as previously reported.[37] ^{1}H NMR spectra were recorded on Bruker 400 Ultra Shield spectrometer. Size exclusion chromatography (SEC) was conducted on a Waters 717 plus autosampler equipped with a Waters 515 pump and a Waters 2414 refractive index (RI) detector. Three columns; Styragel HR0.5 (0-1,000), Styragel HR3 (500-30,000) and a Styragel HR5E (2,000-4,000,000) were applied in sequence for separation. Tetrahydrofuran was used as the eluent at 0.3 mL/min, molecular weights were determined against poly(styrene) standards. The polydispersity index (PDI) obtained from SEC (in THF) is defined as 'M_w/M_n' with the lower limit = 1. Static light scattering analysis was completed on a Viscotek Triple Detector Array (TDA) 302 equipped with a Refractive Index (RI) detector, Viscometer, Right Angle (90°) Light Scattering (RALS) and Low Angle (7°) Light Scattering (LALS). Separation was performed using two PLgel 5 µm Mixed-B columns connected in series. Samples were injected at a volume of 100 µL and eluted through the system at flow rate of 1.0 mL/min in THF. A temperature of 30 °C was maintained during separation and detection. Poly(styrene) 210 kDa was used as calibration for absolute molecular weight determination by Light Scattering. Deionized (DI) water was prepared using an AquaMAX-Basic 321 DI water purification system. Hydrodynamic diameter values were determined by dynamic light scattering (DLS) analysis on a Malvern Zetasizer Nanoseries from Malvern Instruments at 25 °C, each data point is repeated 5 times with each measurement comprised of 15 runs at 30 seconds per run. The measurements were performed on aqueous nanoparticles solutions with concentrations of 3 mg/mL. The polydispersity index (PDI) obtained from DLS (in aqueous media) is defined as 'a dimensionless measure of the broadness of the size distribution calculated from the cumulants analysis' with the lower limit = 0. UV-vis analysis was performed on a Shimadzu UV-2700, Indomethacin concentrations were determined against a calibration curve of solutions of known concentration in EtOH.

Synthesis of Hyperbranched Polymers (HB1-HB4)

Hyperbranched polymers (**HB1-4**) were synthesized by the follow procedure. All experiments were conducted with constant monomer and solvent concentration with varying amounts of RAFT chain transfer agent, radical initiator and cross-linker relative to 15 mmol DEAEMA (Table 1). In a typical synthesis (**HB1**) the RAFT chain transfer agent 4-((((2-carboxyethyl)thio)carbonothioyl)thio)-4-cyanopentanoic acid (184 mg, 0.6 mmol, 1 eq), di(ethylene glycol) dimethacrylate (238 mg, 1.2 mmol, 2 eq), 2-(diethylamino)ethyl methacrylate (2.78 g, 15 mmol, 25 eq) and azobisisobutyronitrile (9.8 mg, 60 µmol, 0.1 eq) were transferred into a 25 mL Schlenk flask fitted with a magnetic stirrer bar and *N,N*'-dimethylformamide (2.8 g) added. The reaction mixture was degassed via three freeze-pump-thaw cycles and backfilled with N_2. The reaction was heated to 70 °C and stirred at 500 rpm for 16 h, after this time NMR analysis was used to determine monomer conversion. The reaction was quenched by rapid cooling, and the polymer purified by three precipitations from THF into pentane. The purified polymer was isolated as a yellow waxy solid. ^{1}H NMR ($CDCl_3$): δ 4.70 (br, C(O)OCH_2CH$_2$O), 4.00 (br, C(O)OCH_2CH$_2$N), 3.63 (br, C(O)OCH$_2$CH_2O), 2.71 (br, CH$_2$CH_2N), 2.58 (br, N(CH_2CH$_3$)$_2$), 1.84 (br, CH_2C(CH$_3$)), 1.04 (br, N(CH$_2$CH_3)$_2$), 0.88 (br, CH$_2$C(CH_3)).

Synthesis of Star Hyperbranched Polymers (SHB1-4)

Star hyperbranched polymers (**SHB1-4**) were synthesized by the follow chain-extension procedure. All experiments were conducted with constant concentrations of hyperbranched polymer precursor, monomer, solvent and radical initiator (Table 2). In a typical synthesis (**SHB1**) the hyperbranched polymer precursor (**HB1**, 0.68 g, 0.125 mmol, 1 eq), oligo(ethylene glycol) methyl ether methacrylate (3.0 g, 10 mmol, 80 eq) and azobisisobutyronitrile (2.1 mg, 12.5 µmol, 0.1 eq) were transferred into a 25 mL Schlenk flask fitted with a magnetic stirrer bar and *N,N*'-dimethylformamide (11.0 g) added. The reaction mixture was degassed via three freeze-pump-thaw cycles and backfilled with N_2. The reaction was heated to 70 °C and stirred at 500 rpm for 16 h, after this time NMR analysis was used to determine monomer conversion. The reaction was quenched by rapid cooling, and the polymer purified by three precipitations from THF into pentane. The purified polymer was isolated as a yellow oil. ^{1}H NMR ($CDCl_3$): δ 4.07 (br, C(O)OCH_2CH$_2$N and C(O)OCH_2CH$_2$O), 3.65 (br, (CH_2CH_2O)$_n$), 3.54 (br, CH_2OCH$_3$), 3.37 (br, CH$_2$OCH_3), 2.95-2.65 (br, CH$_2$CH_2N and N(CH_2CH$_3$)$_2$), 1.81 (br, CH_2C(CH$_3$)), 1.14 (br, N(CH$_2$CH_3)$_2$), 0.87 (br, CH$_2$C(CH_3)).

Synthesis of Linear Polymer (LP1)

RAFT chain transfer agent 4-((((2-carboxyethyl)thio)carbonothioyl)thio)-4-cyanopentanoic acid (92 mg, 0.3 mmol, 1 eq), 2-(diethylamino)ethyl methacrylate (2.78 g, 15 mmol, 50 eq) and azobisisobutyronitrile (4.9 mg, 30 µmol, 0.1 eq) were transferred into a 25 mL Schlenk flask fitted with a magnetic stirrer bar and *N,N*'-dimethylformamide (2.8 g) added. The reaction mixture was degassed via three freeze-pump-thaw cycles and backfilled with N_2. The reaction was heated to 70 °C and stirred at 500 rpm for 16 h, after this time NMR analysis confirmed a conversions of 99 %. The reaction was quenched by rapid cooling, and the polymer purified by three precipitations from THF into pentane. The purified polymer was isolated as a yellow waxy solid. ^{1}H NMR ($CDCl_3$): δ 4.01 (br, C(O)OCH_2CH$_2$N), 2.71 (br, CH$_2$CH_2N), 2.59 (br, N(CH_2CH$_3$)$_2$), 1.84 (br, CH_2C(CH$_3$)), 1.05 (br, N(CH$_2$CH_3)$_2$), 0.89 (br, CH$_2$C(CH_3)).

Synthesis of Diblock Polymer (DB1)

The linear polymer precursor (**LP1**, 1.16 g, 0.125 mmol, 1 eq), oligo(ethylene glycol) methyl ether methacrylate (3.0 g, 10 mmol, 80 eq) and azobisisobutyronitrile (2.1 mg, 12.5 µmol, 0.1 eq) were transferred into a 25 mL Schlenk flask fitted with a magnetic stirrer bar and *N,N*'-dimethylformamide (11.0 g) added. The reaction mixture was degassed via three freeze-pump-thaw cycles and backfilled with N_2. The reaction was heated to 70 °C and stirred at 500 rpm for 16 h, after this time NMR analysis confirmed conversions of 92 %. The reaction was quenched by rapid cooling, and the polymer purified by three precipitations from THF into pentane. The purified polymer was isolated as a yellow oil. ^{1}H NMR ($CDCl_3$): δ 4.07 (br, C(O)OCH_2CH$_2$N and C(O)OCH_2CH$_2$O), 3.65 (br, (CH_2CH_2O)$_n$), 3.54 (br, CH_2OCH$_3$), 3.37 (br, CH$_2$OCH_3), 3.15-2.85 (br, CH$_2$CH_2N and N(CH_2CH$_3$)$_2$), 1.83 (br, CH_2C(CH$_3$)), 1.26 (br, N(CH$_2$CH_3)$_2$), 0.93 (br, CH$_2$C(CH_3)).

Synthesis of Degradable Linear Polymers (LP2-6) and Degradable Hyperbranched Polymer (HB5-8)

Degradable linear and hyperbranched polymers (**LP2-6** and **HB5-8**) were synthesized by the follow procedure. All experiments were conducted with varying ratios of monomers, RAFT chain transfer agent and radical initiator relative to 7.5 mmol of MDO. Reagent ratios are summarized in Table 3. In a typical synthesis (**LP5**) the RAFT chain transfer agent 2-cyano-2-propyl dodecyl trithiocarbonate (27.3 mg, 75 µmol, 1 eq), 2-(diethylamino)ethyl methacrylate (1.39 g, 7.5 mmol, 100 eq), 2-methylene-1,3-dioxepane (0.86 g, 7.5 mmol, 100 eq) and azobisisobutyronitrile (6.1 mg, 37.5 µmol, 0.5 eq) were transferred into a 25 mL Schlenk flask (previously rinsed with Et_3N and dried under high vacuum) fitted with a magnetic stirrer bar and *N,N*'-dimethylformamide (2.5 g) added. The reaction mixture was degassed via three freeze-pump-thaw cycles and backfilled with N_2. The reaction was heated to 70 °C and stirred at 500 rpm for 16 h, after this time NMR analysis was used to determine monomer conversion. The reaction was quenched by rapid cooling, and the polymer purified by three precipitations from THF into pentane. The purified polymer was isolated as a yellow waxy solid. Fully annotated ^{1}H NMR spectra are available in the electronic supplementary information (Fig. S8 and Fig. S10) and Fig. 5.

Synthesis of Degradable Diblock Polymer (DB2) and Degradable Star Hyperbranched Polymer (SHB5-8)

Degradable diblock and star hyperbranched polymers (**DB2** and **SHB5-8**) were synthesized by the following chain-extension procedure. All experiments were conducted with constant ratios of linear (**LP6**) or hyperbranched polymer (**HB5-8**) precursor, monomers, solvent and radical initiator. Reagent ratios are summarized in Table 3. In a typical synthesis (**DB2**) the linear polymer precursor (**LP6**, 0.69 g, 63 µmol, 1 eq), oligo(ethylene glycol) methyl ether methacrylate (1.50 g, 5.0 mmol, 80 eq), 2-methylene-1,3-dioxepane (0.86 g, 7.5 mmol, 120 eq) and

azobisisobutyronitrile (5.1 mg, 31 µmol, 0.5 eq) were transferred into a 25 mL Schlenk flask (previously rinsed with Et_3N and dried under high vacuum) fitted with a magnetic stirrer bar and *N,N*'-dimethylformamide (3.0 g) added. The reaction mixture was degassed via three freeze-pump-thaw cycles and backfilled with N_2. The reaction was heated to 70 °C and stirred at 500 rpm for 16 h, after this time NMR analysis was used to determine monomer conversion. The reaction was quenched by rapid cooling, and the polymer purified by three precipitations from THF into pentane. The purified polymer was isolated as a yellow waxy solid. Fully annotated ^{1}H NMR spectra are available in the electronic supplementary information (Fig. S12) and Fig.5.

pH-Responsive Investigation

Aqueous solutions of star hyperbranched polymers (**SHB1-4** and **SHB7-8**) and linear diblock polymers (**DB1-2**) were prepared by adding 8 mL DI H_2O to 30 mg of polymer, the pH was adjusted and maintained at 5.0 with small aliquots of 1M $HCl_{(aq)}$) during polymer dissolution. After the polymer is fully dissolved DI H_2O is added until the total volume reaches 10 mL. Small aliquots of 1M $HCl_{(aq)}$ and 1M $NaOH_{(aq)}$ were used to adjust the pH values from 5.0 to 9.0. pH values were determined using a Mettler Toledo S220 pH probe. Dynamic light scattering measurements were performed at regular intervals cycling between pH 5.0 and 9.0.

Indomethacin Solubilization and pH-Triggered Release

200 mg of star hyperbranched polymer **SHB2** (or linear diblock polymer **DB1**) and 100 mg Indomethacin (IMC) were dissolved in 10 mL EtOH, and 10 mL DI water added slowly. EtOH was evaporated at room temperature under constant stirring at 500 rpm. The obtained solution was filtered to remove the excess IMC and UV-vis was used to determine the % of IMC in solution. The 10 mL aqueous solution obtained was split into two stock solutions, one 5 mL solution was maintained at pH 6.5 and the second 5 mL solution adjusted to and maintained at pH 4.5. pH adjustments were made using small aliquots of 1M $HCl_{(aq)}$ and 1M $NaOH_{(aq)}$. At specific time points small samples were extracted and centrifuged to isolate the precipitated IMC from the IMC/polymer solution. 30 µL of the supernatant was taken out and dissolved in 2.97 mL EtOH for UV-vis analysis, against a calibration curve of known IMC concentrations in EtOH, the remaining solution was replenished with 30 µL H_2O at pH 4.5 or 6.5 and added back to the respective IMC/polymer solutions.

Thiol Functionalization of Star Hyperbranched Polymer via Aminolysis

The thiol chain end-functional star hyperbranched polymer (**SHB2-SH**) was synthesized by the follow procedure. Trithiocarbonate chain end-functionalized star hyperbranched polymer (**SHB2**, 2.31 g, approx. 0.07 mmol of trithiocarbonate end-group, 1 eq) was dissolved in THF (10 mL) and transferred to a Schlenk flask fitted with a rubber septum. The solution was degassed via three freeze-pump-thaw cycles and backfilled with N_2. 3-Amino-1-propanol (0.26 g, 3.50 mmol, 50 eq) was added via syringe and the reaction was heated to 45 °C for 2 h. After this time the reaction was purified by two precipitations from THF into hexane. The polymer was isolated as a clear oil. Aminolysis was confirmed by UV-vis (3 mg/mL in THF) of **SHB2** compared with **SHB2-SH**. The process was performed under identical conditions with the linear diblock polymer (**DB1**) to afford the thiol end-functionalized **DB1-SH**.

Conjugation of Fluorescein via Thiol-ene Click Chemistry

SHB2-SH (0.2 g, approx. 6.0 µmol of thiol end-group, 1 eq) and *N*-(5-Fluoresceinyl)maleimide (3.0 mg, 7.0 µmol, 1.2 eq) were dissolved in DMF (2 mL), the reaction was stirred for 20 h at room temperature in the dark. The polymer obtained was purified by dialysis against H_2O in a 5 mL Float-A-Lyzer (M_w cut-off 8-10 kDa) for 24 h. After removal of water via freeze-drying, the desired polymer (**SHB2-Dye**) was obtained as a red oil. Successful dye conjugation was confirmed by UV-vis (3 mg/mL in H_2O) of **SHB2-Dye** compared with **SHB2** and **SHB2-SH**.

Gelation of Thiol Functional End-Functionalized Star Hyperbranched Polymer

SHB2-SH (150 mg) was dissolved in the minimal amount of acetone required. H_2O (2 mL) was then added followed by H_2O (1 mL) containing 10 µl H_2O_2 (30 % w/w). The solution was left open for 24 h to allow the acetone to evaporate, affording a polymer concentration of 5 wt %. Successful gelation was confirmed by the vial inversion test. The experiment was repeated using different polymer concentrations (10 and 1 wt %). This was achieved by varying the initial volume for H_2O added and keeping the polymer mass and volume of H_2O_2 constant. We observed hydrogel formation at 10 wt % but this could not be achieved at a low polymer concentration of 1 wt %. Control experiments under identical conditions were performed with **SHB2**, **DB1** and **DB1-SH**. The 5 wt % **SHB-SH** hydrogel was disassembled by the addition of 0.5 mL H_2O (0.5 mL) containing tris(2-carboxyethyl)phosphine (80 mg), the aqueous solution containing the reducing agent was added to the surface of the gel and complete disassembly was observed after 48 h.

Ester Hydrolysis and Degradation of Linear, Hyperbranched, Diblock and Star Hyperbranched Polymers

The hydrolysis of each MDO containing polymer (**LP2-6**, **HB5-8**, **DB2** and **SHB5-8**) was performed under accelerated alkali conditions. The conditions previously applied to prepare aqueous solutions for the pH-responsive investigation were repeated resulting in aqueous solutions (3 mg/mL) of each degradable polymer. To a 10 mL solution of each polymer (30 mg) was added a solution of $NaOH_{(aq)}$ (0.08 g in 10 mL H_2O) resulting in a NaOH concentration of 0.1 M. Each solution was heated to 40 °C for 24 h, after this time the obtained oligomer solution was naturalized to pH 7.0 with 1M $HCl_{(aq)}$ and lyophilized. The obtained solid was the analyzed by SEC in THF.

Results and Discussion

Our main focus was to investigate the RAFT polymerization of pH-responsive star hyperbranched (SHB) polymers with the monomer composition OEGMA-*b*-(DEAEMA-*c*-DEGDMA) and to compare their properties to a corresponding linear diblock (DB) polymer able to undergo conventional pH-induced micellization. Initially, we synthesize a series of DEAEMA-*c*-DEGDMA hyperbranched polymers (**HB1-4**) which are subsequently chain-extended with OEGMA affording the OEGMA-*b*-(DEAEMA-*c*-DEGDMA) star hyperbranched polymers (**SHB1-4**). A linear OEGMA-*b*-DEAEMA diblock polymer (**DB1**) analog with identical monomer composition to **SHB2** was then prepared. The uptake and release of Indomethacin facilitated by **SHB2** was compared to **DB1** micelles. A series of experiments incorporating the cyclic ketene acetal monomer MDO within sequential polymerization steps introducing main-chain polyester functionalities into both blocks of star hyperbranched (**SHB5-8**) polymers and a diblock (**DB2**) polymer are then performed. These experiments furnished main-chain degradable schizophrenic stimuli-responsive polymeric materials, which self-assembly in response to either changes in pH or temperature.

Hyperbranched Polymer Synthesis and Characterization (HB1-4)

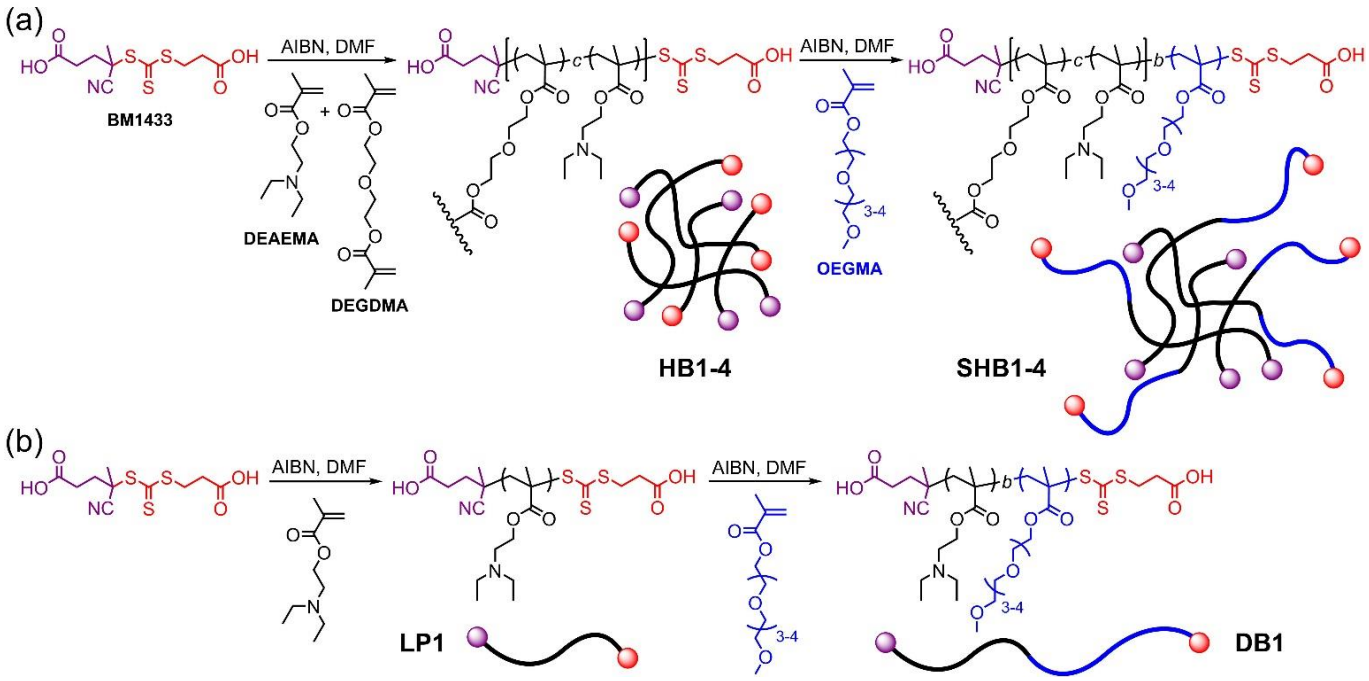

Scheme 1. (a) Synthesis of DEAEMA hyperbranched polymers (**HB1-4**) and their chain-extension with OEGMA to afford star hyperbranched polymers (**SHB1-4**). (b) Synthesis of DEAEMA linear polymer (**LP1**) and its chain-extension with OEGMA to afford the diblock polymer (**DB1**).

The RAFT chain transfer agent 4-((((2-carboxyethyl)thio)carbonothioyl)thio)-4-cyanopentanoic acid (BM1433) was used (Scheme 1) to facilitate the copolymerization of 2-(diethylamino)ethyl methacrylate (DEAEMA) and the divinyl cross-linker di(ethylene glycol) dimethacrylate (DEGDMA) with AIBN as the racial source. This RAFT agent was selected for its potential application in aqueous RAFT polymerization. The ratio of [BM1433]/[DEGDMA] was kept constant at 0.5 for each experiment, as increasing the amount of divinyl cross-linker relative to the RAFT chain transfer agent leads to the undesirable formation of insoluble gels.[30] Instead the amount of DEAEMA relative to the RAFT chain transfer agent was varied, essentially adjusting the cross-linking density along each polymer chain. Four hyperbranched polymers were prepared with ratios of BM1433 to DEAEMA of 1:25, 1:50: 1:100 and 1:200, **HB1-4** respectively. For each experiment the monomer wt % relative to the solvent (DMF) was also kept constant at 50 wt % (15 mmol DEAEMA and 2.8 g of DMF), each experiment proceeded without any undesirable gelation.

Table 1. Synthesis and characterization of RAFT generated DEAEMA-*c*-DEGDMA hyperbranched (**HB1-4**) and DEAEMA linear (**LP1**) polymers.

Sample ID	[DEAEMA] : [DEGDMA] : [BM1433] : [AIBN]	Conv.[a] (%)	M_n^{theo} (g mol^{-1})	M_n[b] (g mol^{-1})	M_w[b] (g mol^{-1})	PDI[b] (M_w/M_n)	M_n[c] SLS (g mol^{-1})	DB	RB
HB1	25 : 2 : 1 : 0.1	99	4,900	5,900	13,200	2.24	82,000	0.135	7.41
HB2	50 : 2 : 1: 0.1	99	9,500	14,000	25,500	1.82	145,000	0.068	14.71
HB3	100 : 2 : 1 : 0.1	96	18,100	11,500	19,000	1.65	165,000	0.035	28.57
HB4	200 : 2 : 1 : 0.1	90	33,700	17,400	31,500	1.81	160,000	0.019	52.63
LP1	50 : 0 : 1 : 0.1	92	9,600	6,600	8,200	1.24	-	-	-

All reactions were performed with 15 mmol of DEAEMA in DMF (2.8 g), at 70 °C for 16 h. [a] Determined by ^{1}H NMR spectroscopy, [b] determined by SEC in THF against PS standards, [c] determined by SEC online static light scattering in THF, M_n^{theo} = theoretical number average molecular weight of linear segments between branching points, DB = degree of branching and RB = average repeat units per branch (1/DB).

The resulting hyperbranched polymers (**HB1-4**) were characterized by ^{1}H NMR spectroscopy, size exclusion chromatography (SEC) with online static light scattering. The details of their synthesis and characterization are displayed in Table 1. Monomer conversion was monitored by ^{1}H NMR spectroscopy, comparing the vinyl protons from DEAEMA (δ 6.07 and 5.53 ppm) and DEGDMA (δ 6.11 and 5.56 ppm) with the DMF solvent peak (δ 8.02 ppm). While the vinyl peaks from DEAEMA and DEGDMA are not distinct enough to determine individual monomer conversions is it clear that both monomers polymerize with similar overall conversions after 16 h. All hyperbranched polymerizations proceeded with over 90 % conversion, high conversions are important in the synthesis of hyperbranched polymers as the probability of branching increases with conversion.

The theoretical number average molecular weight of linear segments between branching points (M_n^{theo}) values displayed in Table 1 are determined from equation 1:

$$M_n^{theo} = \left(\frac{[DEAEMA]}{[BM1433]} \times MW \text{ of DEAEMA} \times Conv.\right) + MW \text{ of BM1433} \qquad (1)$$

Size exclusion chromatography (SEC) analysis (Fig. 1(a-d), dashed lines) in THF displayed a bimodal distribution for **HB1**, whereas **HB2-4** displayed monomodal distributions. The M_n and M_w values determined against poly(styrene) standards are much lower than expected, a common problem when comparing tightly cross-linked branched structures to linear polymer standards. However, the high PDI values (1.81 – 2.24) obtained are consistent with the synthesis of hyperbranched polymers prepared by copolymerization with a divinyl monomer. Absolute M_n values obtained by online static light scattering displayed much high values confirming the preparation of cross-linking macromolecules. As the ratio of DEAEMA to RAFT chain transfer agent increased static light scattering analysis displayed an overall trend towards increased molecular weight from **HB1** to **HB4**, with **HB3** possessing a slightly higher molecular weight that **HB4**. This could potentially be due to differences in conversion. **HB3** reached 96 % conversion compared to 90 % for **HB4**, this increase in conversion would significantly increase the probability of cross-linking. Hyperbranched polymers are further analyzed by ^{1}H NMR spectroscopy (ESI, Fig. S1) to determine the degree of branching (DB), which describes the fraction of branching units in each macromolecule. Equation 2 is used to determine the DB, which describes the DB in relation to the number of terminal (T), linear (L) and branching (B) units:[59]

$$DB = \frac{B + T}{B + T + L} \qquad (2) \qquad DB = \frac{B + R + Z}{B + R + Z + L} \qquad (3) \qquad DB = \frac{B + 2R}{B + 2R + L} \qquad (4)$$

When RAFT polymerization is employed to prepare hyperbranched polymers the terminal groups originate from the chain transfer agent R-group (R) and Z-group (Z), so equation 2 can be modified to give equation 3. In our experiments the presence of the terminal Z-groups are not visible by ^{1}H NMR spectroscopy, however, as the number of Z-groups and R-groups are approximately equal equation 3 can be further modified to give equation 4.[34] Linear (non-cross-linking) polymers have a DB close to zero and perfectly branched structure have a DB = 1. By comparing the integrals (ESI, Fig. S2) of the terminal R-group (R) protons (–C*H*$_2$COOH–) at 2.33 ppm, the DEGDMA (B) protons (CH$_2$C*H*$_2$O) at 3.63 ppm and the DEAEMA (L) protons (C*H*$_2$CH$_2$N) at 4.00 ppm it is possible to derive the degree of branching for each DEAEMA-*b*-DEGDMA hyperbranched polymer (Table 1) and subsequently the average repeat units per branch (RB) which is equal to 1/DB. The degree of branching increases from 0.019 (**HB4**) to 0.135 (**HB1**) as the initial feed ratio of [DEAEMA]/ [DEGDMA] increases from 100 to 12.5. Taken together the data obtained from ^{1}H NMR spectroscopy and SEC confirms the successful preparation of hyperbranched polymers.

Star Hyperbranched Polymer Synthesis and Characterization (SHB1-4)

Each hyperbranched polymer **HB1-4** was chain-extended with OEGMA, affording star hyperbranched polymers **SHB1-4**, respectively. The ratio of hyperbranched macro-RAFT chain transfer agent to OEGMA was kept constant at 1:80 for each experiment. The resulting star hyperbranched polymers (**SHB1-4**) were characterized by ^{1}H NMR spectroscopy and size exclusion chromatography (SEC). The details of their synthesis and characterization are displayed in Table 2. Monomer conversion was monitored by ^{1}H NMR spectroscopy, comparing the vinyl protons from OEGMA (δ 6.07 and 5.52 ppm) with the DMF solvent peak (δ 8.02 ppm). Each chain-extension proceeded with over 95 % conversion. Size exclusion chromatography (SEC) analysis (Fig. 1(a-d), solid lines) in THF displayed successful chain-extensions and monomodal distributions for each experiment confirming retention of the trithiocarbonate functionality after purification of the corresponding hyperbranched polymer. Again, comparing branched polymers with linear calibration standards does not yield accurate molecular weight values so absolute M_n values where obtained by online static light scattering, it was then possible to calculate the number of arms per star hyperbranched polymer using equation 5:

$$\text{no. of arms} = \frac{M_n \text{ of } \mathbf{SHB} \text{ polymer} - M_n \text{ of } \mathbf{HB} \text{ precursor}}{M_n^{theo} \text{ of poly(OEGMA) block}} \qquad (5)$$

The theoretical M_n of the poly(OEGMA) block was calculated from the OEGMA monomer conversion, the feed ratio of hyperbranched polymer to OEGMA and the molecular weight of OEGMA. **SHB1** displayed the largest number of arms as it was synthesized via the chain-extension of **HB1** which possessed the highest cross-linking density and subsequently the highest wt % of trithiocarbonate Z-groups functionality per hyperbranched polymer. Conversely, **SHB4** displayed the lowest number of arms as it was synthesized via the chain-extension of **HB4** which possessed the lowest cross-linking density and subsequently the lowest wt % of trithiocarbonate RAFT Z-group functionality per polymer.

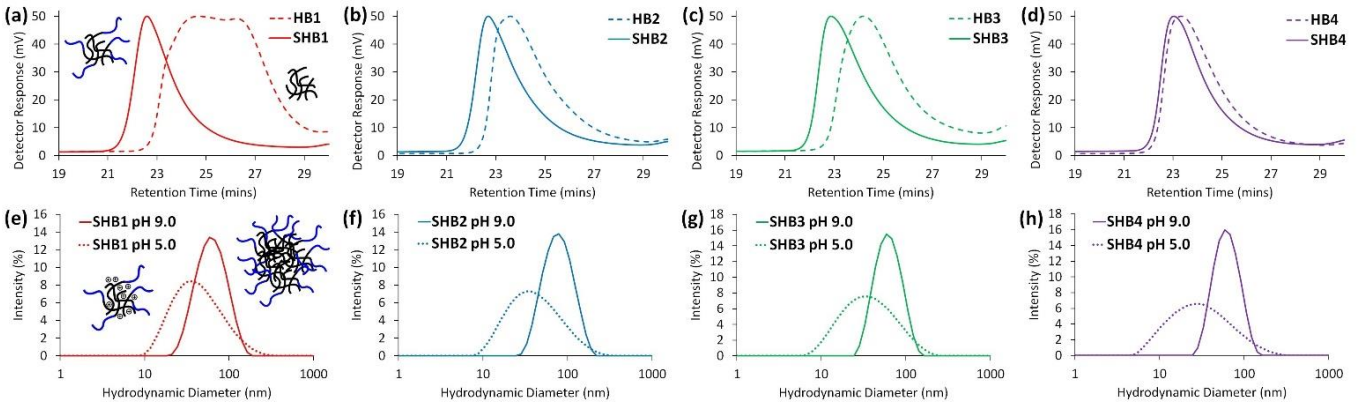

Fig. 1 (a-d) SEC refractive index traces (in THF) of hyperbranched polymers **HB1-4** (dashed lines) and their subsequent chain-extension to the corresponding star hyperbranched polymer **SHB1-4** (solid lines). (e-f) DLS analysis in H_2O (pH 5.0 and 9.0) of star hyperbranched polymers **SHB1-4** (3 mg/mL) at pH 5.0 (dotted lines) and pH 9.0 (solid lines).

Table 2. Synthesis and characterization of RAFT generated DEAEMA-*b*-OEGMA star hyperbranched polymers (**SHB1-4**) and DEAEMA-*b*-OEGMA linear diblock polymer (**DB1**).

Sample ID	[OEGMA] : [Macro-RAFT] : [AIBN]	Conv.[a] (%)	M_n[b] (g mol^{-1})	M_w[b] (g mol^{-1})	PDI[b] (M_w/M_n)	M_n[c] SLS (g mol^{-1})	*no. of arms*	D_h[d] pH 5.0	PDI[d] pH 5.0	D_h[d] pH 9.0	PDI[d] pH 9.0
SHB1	80 : 1 (**HB1**): 0.1	95	31,500	65,100	2.07	380,000	13.1	54 nm	0.281	63 nm	0.167
SHB2	80 : 1 (**HB2**): 0.1	96	23,800	53,000	2.23	366,000	9.6	58 nm	0.381	81 nm	0.174
SHP3	80 : 1 (**HB3**): 0.1	96	21,300	43,200	2.03	259,000	4.1	44 nm	0.280	64 nm	0.125
SHB4	80 : 1 (**HB4**): 0.1	96	21,400	39,100	1.83	244,000	3.65	48 nm	0.396	65 nm	0.117
DB1	80 : 1 (**LP1**): 0.1	92	23,200	29,500	1.27	-	-	24 nm	0.290	54 nm	0.122

All reactions were performed with 10 mmol OEGMA in DMF (11.0 g), at 70 °C for 16 h. [a] Determined by ^{1}H NMR spectroscopy, [b] determined by SEC in THF against PS standards, [c] determined by SEC online static light scattering in THF, [d] determined by dynamic light scattering in H_2O (3 mg/mL).

After purification by precipitation ^{1}H NMR spectroscopy (ESI, Fig. S3) was used to confirm the ratio of DEAEMA monomer units to OEGMA monomer units within each SHB polymer. The data obtained was consistent with the monomer conversions obtained during the both polymerization steps.

Star Hyperbranched Polymer pH-Responsive Investigation

Our next goal was to examine the pH-responsive properties of the star hyperbranched polymer series **SHB1-4**. Our primary aim was to probe the effect of core cross-linking density on pH-responsive behavior. However, as the ratio of RAFT agent to DEGDMA is fixed and the molar equivalence of DEAEMA is adjusted during the synthesis of **HB1-4**, we are also altering the ratio of DEAEMA: OEGMA (after chain-extension). Consequently, at high pH the ratio of hydrophobic core to hydrophilic corona is also varied from **SHB1** (higher OEGMA content) to SHB4 (lower OEGMA content). Dynamic light scattering analysis (Fig.1 (e-h) and Table 2) at pH 5.0 displayed relatively large PDIs (0.280 – 0.396) and hydrodynamic diameters in the range of D_h = 44 – 58 nm, seemingly at low pH **SHB1-4** are discrete nanoparticles with fully protonated DEAEMA cores. After pH adjustment to 9.0 each star hyperbranched polymer displayed an increase in size (D_h = 63 – 81 nm) and a decrease in PDI (0.117 – 0.174). This data suggests the star hyperbranched polymers are self-assembling, upon tertiary amine deprotonation, at high pH into star hyperbranched 'micelles' a similar observation was reported[26] by the Sumerlin group with changes in solvent. **SHB1** (D_h = 54 nm) and **SHB2** (D_h = 58 nm) displayed larger hydrodynamic diameters relative to **SHB3** (D_h = 44 nm) and **SHB4** (D_h = 48 nm) at pH 5.0, this is likely due to their relatively larger number of linear arms and higher cross-linking densities. **SHB1** displays the smallest increase in size upon deprotonation (D_h = 54 to 63 nm). This is presumably due to a lower ratio of hydrophobic core molecular weight relative to the hydrophilic corona. With a lower hydrophobic content self-assembly might not be required to such a high degree in order for **SHB1** to remain in solution. **SHB3** and **SHB4** displayed more significant size increases at pH 9.0 (D_h = 44 to 64 nm and D_h = 48 to 65 nm, respectively) conversely this is could be due to the relatively larger hydrophobic core molecular weight relative to the hydrophilic corona. **SHB2** showed the most significant size increase upon self-assembly (D_h = 58 to 81 nm). A more detailed pH study (Fig. 2 (a)) suggests that the core of **SHB2** contracts at pH 6.0 before self-assembly at pH 7.0. Most probably at pH 6.0 partial core deprotonation occurs which expels water from the core resulting in contraction. This was not observed for **SHB1**, **SHB3** and **SHB4**. We hypothesize that this interesting observation is unique to **SHB2** because **SHB1** is too densely cross-linked, whereas **SHB3** and **SHB4** are too loosely cross-linked for contraction to occur. These results confirm that the pH-responsive self-assembly is related to the cross-linking density within the hyperbranched core and the hydrophobic-hydrophilic ratio after deprotonation.

As **SHB2** undergoes an initial core contraction at pH 6.0 and then aggregates to a larger extend than the other SHB polymers it was decided that this structure possessed the most interesting pH-responsive behavior, consequently **SHB2** was selected for further investigation. With the aim of comparing the properties of this star hyperbranched polymer to a conventional diblock polymer the corresponding linear diblock polymer (**DB1**) with an identical composition ($DEAEMA_{50}$:$OEGMA_{80}$) to **SHB2** was synthesized (Scheme 1). Initially, a linear $DEAEMA_{50}$ polymer (**LP1**) was prepared, this polymer displayed a lower molecular weight and PDI when compared to its hyperbranched polymer **HB2**

counterpart (Table 1), confirming RAFT control. This polymer was then chain-extended with OEGMA affording **DB1** which also displayed a lower molecular weight and PDI compared to its star hyperbranched polymer **SHB2** counterpart (Table 2). Size exclusion chromatography (ESI, Fig. S4(a)) confirmed a successful chain extension and dynamic light scattering analysis (ESI, Fig. S4(b) and Table 2) confirmed that **DB1** is a soluble unimolecular linear polymer (D_h = 24 nm) at pH 5.0 and subsequently self-assembles at pH 9.0 (D_h = 54 nm) into a conventional micelle. Directly comparing the pH-responsiveness of **SH2** with **DB1** (Fig. 2(b)) clearly shows that the incorporation of cross-linking during the first polymerization step results in a significant increase in size at pH 5.0 and after self-assembly at 9.0. From the combined SEC, DLS and ^{1}H NMR data it can be concluded that the cross-linking during the first polymerization step successfully links multiple growing chains together furnishing hyperbranched polymers which are then chain-extended affording star hyperbranched polymers.

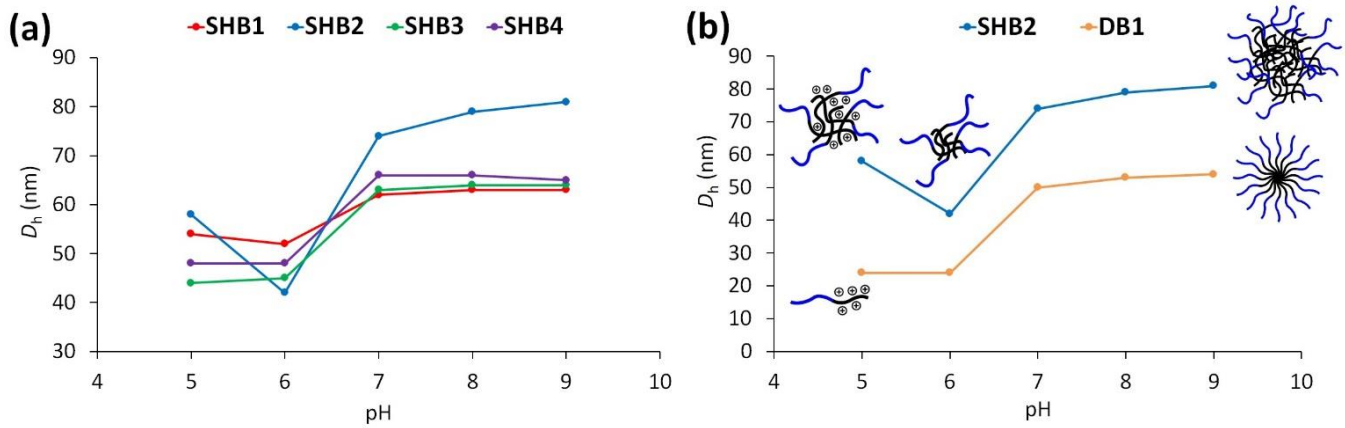

Fig. 2 (a) pH-Responsive behavior of star hyperbranched polymers **SHB1-4** in H_2O (3 mg/mL). (b) pH-Responsive behavior of star hyperbranched polymer **SHB2** and corresponding diblock polymer **DB1** in H_2O (3 mg/mL).

Uptake and Release of Hydrophobic Active (SHB2 and DB1)

Even though the addition of cross-linking during the first polymerization step does not significantly increase experimental complexity it is necessary to demonstrate the benefit of synthesizing a SHB polymer compared to analogous linear DB polymer. With this in mind we investigated the ability of the **SHB2** and **DB1** to uptake the hydrophobic pharmaceutical active Indomethacin (IMC). 200 mg of **SHB2** and **DB1** were separately dissolved in EtOH (10 mL) and IMC (100 mg) added. DI H_2O (10 mL, pH 7.0) was added slowly and EtOH allowed to evaporate while stirring at room temperature. After 24 h the excess Indomethacin was removed by filtration and a small sample (30 µL) of each aqueous solution was extracted, diluted with EtOH (2.97 mL), and the % uptake of IMC determined by UV-vis spectroscopy against an IMC in EtOH (+ 1 % H_2O by volume) calibration curve (ESI, Fig. S5(a)). A control experiment was conducted under identical conditions without the presence of either **SHB2** or **DB1**, UV-vis could not detect the presence of IMC in H_2O after filtration (ESI, Fig. S5(b)). We observed that **SHB2** was able to uptake 90 % of the initial IMC added while **DB1** was only able to uptake 48 % of initial IMC (Fig. 3(a)). As the initial feed ratio of polymer to drug was 2: 1 the resulting wt % uptake of drug relative to polymer was therefore 45 wt % for **SHB2** and 24 wt % for **DB1**. The difference in IMC uptake and release between **SHB2** and the control experiments can be clearly observed visually (ESI, Fig. S6). These experiments indicate the improved uptake ability of the star hyperbranched polymer micelles relative to a corresponding conventional diblock micellar assembly. We believe the significant variance is due to the difference in polymeric structure, the conventional micelles of **DB1** are likely more ordered with tightly packed polymer chains. Whereas the presence of branching points in the core of **SHB2** inhibits close packing of polymer chains and introduces more randomness and potentially larger voids which could facilitate an increase in uptake of the active.

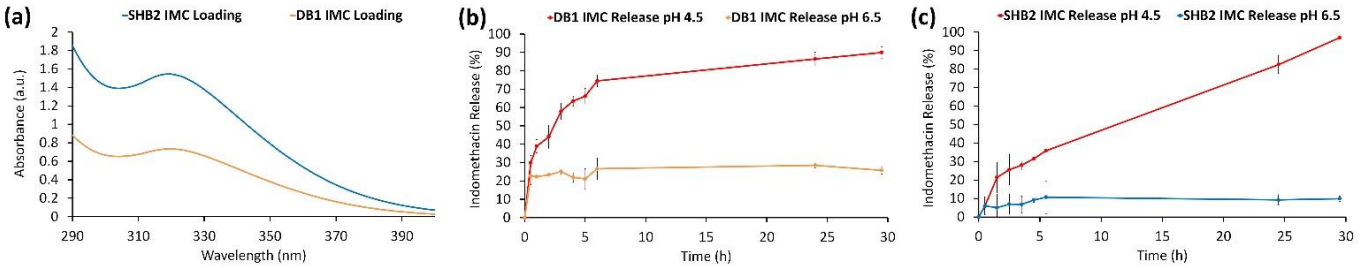

Fig. 3 (a) Loading of Indomethacin (IMC) within star hyperbranched polymer **SHB2** and corresponding diblock polymer **DB1** under identical conditions, and subsequent release of Indomethacin at pH 4.5 and 6.5 from (b) diblock polymer **DB1** and (c) star hyperbranched polymer **SHB2**.

Each aqueous polymer (**SHB2** and **DB1**)/ IMC solution was then divided into two portions and the pH of one adjusted to 6.5 while the other was adjusted to 4.5. Each solution was maintained at either pH 6.5 or 4.5 with small aliquots of 1M $HCl_{(aq)}$ or 1M $NaOH_{(aq)}$ while the active release monitored by UV-vis. The release of IMC from **DB1** at pH 6.5 was reached approx. 25 %, whereas the release at pH 4.5 proceeded quickly reaching 80 % after 6 h (Fig. 3(b)) due to micelle disassembly. The release of IMC from **SHB2** at pH 6.5 was negligible, conversely the release at pH 4.5 reached 35 % after 6 h and 80 % after 24 h. Each release profile was repeated in triplicate and the standard deviation displayed in error bars (Fig. 3(b) and (c)). Both **SHB2** and **DB1** samples at pH 6.5 were very stable for up to two weeks displaying no additional

Indomethacin release. After this time we began to observe some polymer and Indomethacin precipitation. The significantly slower release profile observed at pH 4.5 for **SHB2** is likely due to IMC remaining within the cross-linked hyperbranched core after disassembly, before leeching out. These uptake and release experiments demonstrate the ability of star hyperbranched polymers to improve loading and slow down release rates, both of which are highly advantageous properties in various applications.

Post-Polymerization Functionalization and Gelation

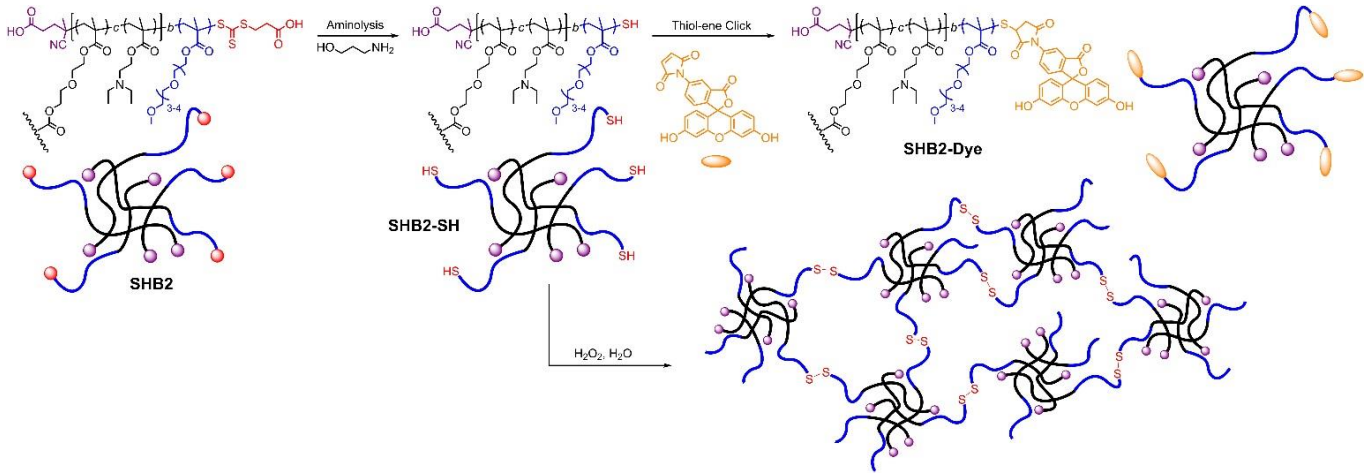

Scheme 2. Aminolysis of RAFT trithiocarbonate Z-group located at star hyperbranched polymer periphery to a primary thiol, followed by either post-polymerization functionalization via thiol-ene click chemistry or gelation via disulfide formation under oxidative conditions.

An attractive property of RAFT polymerization is the ability to introduce additional functionality via post-polymerization Z-group cleavage to a primary thiol. This synthetic route has been exploited to introduce fluorescein dye via thiol-ene click chemistry and gelation via disulfide bond formation at the periphery of **SHB2-SH** (Scheme 2). **SHB2** was treated with 3-amino-1-propanol (approx. 50 eq per z-group) in THF, under N_2, at 45 °C for 2 h. After purification by precipitation UV-vis spectroscopy (in THF) confirmed the successful cleavage of the trithiocarbonate functionality affording **SHB2-SH** (Fig. 4(a)). This was repeated under identical conditions to convert **DB1** to **DB1-SH**. In order to confirm the presence of the reactive thiol site **SHB2-SH** was coupled to *N*-(5-Fluoresceinyl)maleimide (1.2 eq excess) in DMF. After stirring for 20 h dialysis against DI H_2O was carried out for 24 h to remove any excess *N*-(5-Fluoresceinyl)maleimide before UV-vis spectroscopy (in H_2O) confirmed the successful coupling of the fluorescein dye (Fig. 4(b)). This experiment demonstrates the potential to introduce specific functionalities post-polymerization, which could be very beneficial for targeting or bio-imaging applications.

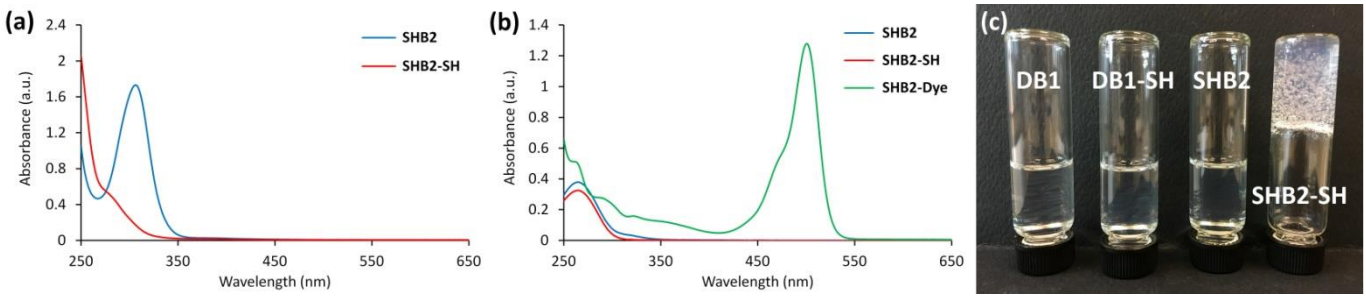

Fig. 4 (a) Aminolysis of **SHB2** RAFT trithiocarbonate Z-group, confirmed by UV-vis (in THF) affording **SHB2-SH**, (b) functionalization of **SHB-SH** with *N*-(5-Fluoresceinyl)maleimide via thiol-ene click chemistry, confirmed by UV-vis (in H_2O) affording **SHB2-Dye** and (c) gelation of **SHB2-SH** under oxidative conditions.

If the proposed star morphology of **SHB2** is indeed accurate, the star hyperbranched polymer **SHB2-SH** would possess multiple thiol functionalities at the periphery of each nanoparticle. This multivalency could be used to cross-link multiple SHB polymers together through disulfide bond formation, under oxidative conditions. This was achieved at a polymer concentration of 5 wt % in the presence of H_2O_2 (Fig. 4(c). 150 mg of **DB1**, **DB1-SH**, **SHB2** and **SHB2-SH** were dissolved in approx. 0.2 mL of acetone followed by the addition of H_2O (2 mL) each sample was stirred to ensure even polymer distribution. To each sample H_2O (1 mL) containing 10 µL H_2O_2 (30 % w/w) was added, and the final solutions (5 wt % polymer) were left to stand open to the atmosphere to allow the acetone to evaporate for 24 h. The vial inversion test confirmed that **DB1**, **DB1-SH** and **SHB2** showed no hydrogel formation, whereas **SHB2-SH** clearly formed a macroscopic hydrogel. The **SHB2-SH** hydrogel formation was also achieved at a higher polymer concentration of 10 wt %, unfortunately this could not be repeated at a lower polymer concentration of 1 wt % (ESI, Fig. S7). The **SHB2-SH** hydrogel can easily be disassembled via disulfide bond reduction after addition of an aqueous solution containing an excess of tris(2-carboxyethyl)phosphine. Taken together these experiments further confirm the star morphology of the SHB polymers synthesized and the presence of multiple peripheral thiol functionalities after RAFT Z-group cleavage.

Incorporation of Main-Chain Degradability

Radical ring-opening polymerization (rROP) of cyclic ketene acetals (CKA) (Scheme 3(c)) in combination with methacrylate copolymerization has been employed to incorporate main-chain polyester degradability into the SHB architecture while maintaining pH-responsive behavior. 2-Methylene-1,3-dioxepane (MDO) was selected as it's copolymerization with several methacrylate-based monomers has been reported in the literature.[60, 61] MDO is comparatively less reactive than methacrylate-based monomers, the reactivity ratios for a methyl methacrylate (MMA) and MDO bulk copolymerization have been reported as r_{MDO} = 0.057 and r_{MMA} = 34.12.[62] Typically, an equimolar copolymerization introduces around 20 mol. % of ring-opened MDO within the resulting methacrylate-based copolymer. It was hypothesized that this molar equivalence of MDO incorporation should be sufficient to introduce degradability (into short chain oligomers) while maintaining the pH-responsiveness of poly(DEAEMA). The main challenge encountered was the incorporation of MDO within each polymerization step. Several examples of RAFT-mediated copolymerization of vinyl and CKA monomers have been reported in the literature, however, we were unable to find an example of a block copolymer which possessed a CKA monomer within each block. 2-Cyano-2-propyl dodecyl trithiocarbonate (CPDT) was selected as the RAFT chain transfer agent as the carboxylic acid R- and Z-groups of BM1433 are able to couple to cyclic ketene acetal functionalities via electrophilic addition,[63] an undesirable side reaction.

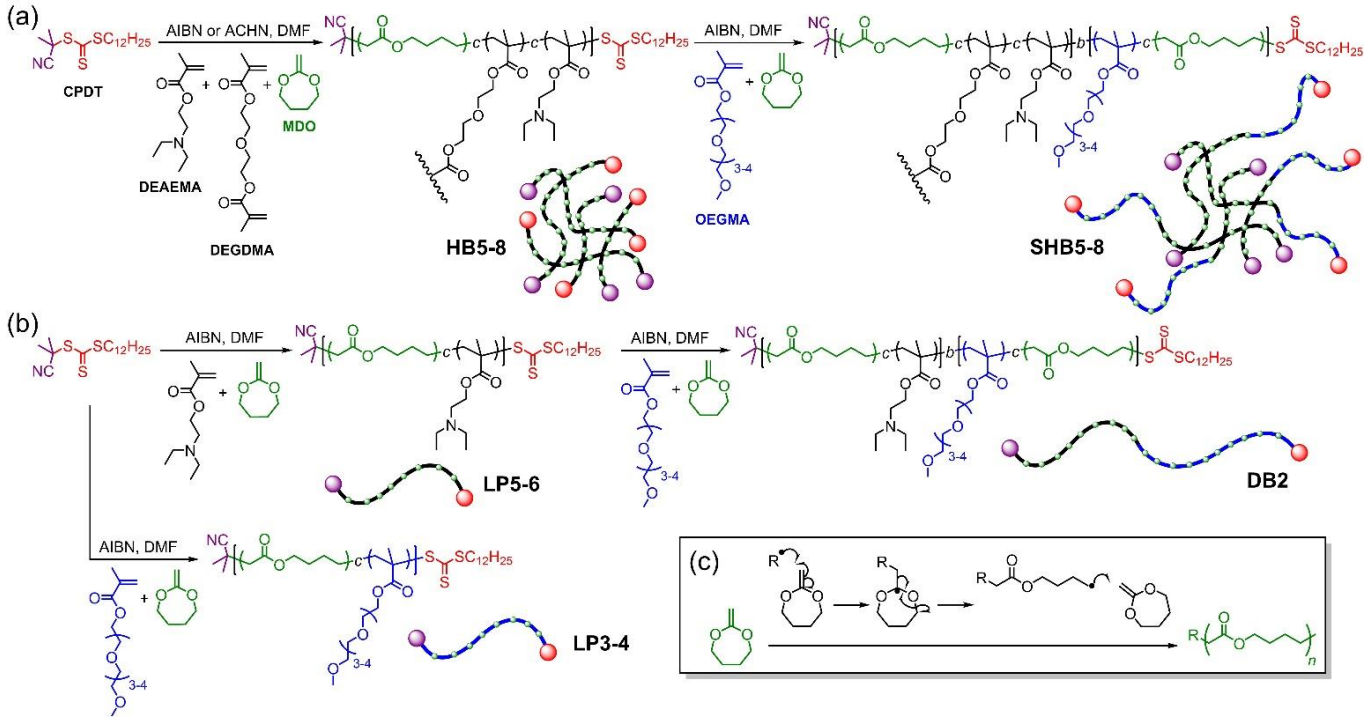

Scheme 3. (a) Synthesis of the MDO containing DEAEMA-based hyperbranched polymers (**HB5-8**) and subsequent chain-extension with MDO and OEGMA to afford the main-chain degradable star hyperbranched polymers (**SHB5-8**). (b) Synthesis of MDO containing OEGAM-based (**LP3-4**) and DEAEMA-based linear polymers (**LP5-6**) and the subsequent chain-extension of **LP6** with OEGMA and MDO to afford the main-chain degradable diblock polymer (**DB2**). (c) MDO radical ring-opening polymerization mechanism.

Initially, a series of DEAEMA or OEGMA-based polymers were synthesized with the incorporation of MDO. Conditions were determined that allowed the chain-extension of poly(DEAEMA-*c*-MDO) with OEGAM and MDO affording diblock polymer **DB2** (Scheme 3 (b)), a degradable analog of **DB1**. Conditions were then found which mediated the ter-polymerization of DEAEMA, DEGDMA and MDO affording in the hyperbranched polymer **HB8**, a degradable analog of **HB2**. This hyperbranched polymer was then chain-extended with OEGMA and MDO affording **SHB8** (Scheme 3 (a)), a degradable analogue of **SHB2**. Conditions for the MDO radical ring-opening polymerizations are outlined in Table 3. A RAFT chain transfer agent to AIBN ratio of 1: 0.5 was employed, this increase in radical concentration is required to facilitate the incorporation of MDO during methacrylate copolymerization. For each experiment the monomer conversions were determined by ^{1}H NMR spectroscopy by comparing the vinyl protons from either DEAEMA or OEGMA (δ 6.07 and 5.52 ppm) and MDO (δ 3.42 ppm) with the DMF solvent peak (δ 8.02 ppm). $CDCl_3$ was passed through Na_2CO_3 prior to use to avoid MDO hydrolysis during ^{1}H NMR analysis. Two OEGMA-*c*-MDO copolymers **LP3** (PDI = 4.45) and **LP4** (PDI = 2.41) were synthesized in the presence of CPDT and AIBN, at 70 °C for 16 h, with varying molar ratios of OEGMA: MDO: CPDT: AIBN (Table 3). After purification ^{1}H NMR spectroscopy (ESI, Fig. S8) was used to determine the composition of MDO within the copolymers, this was done by comparing the integral of the OEGMA terminal -C*H*$_3$ peak at δ 3.36 ppm with the combined integrals of the OEGMA and MDO -C*H*$_2$- peaks at δ 4.0 – 4.2 ppm. In each OEGMA-*c*-MDO experiment the monomer conversions were consistent with the final copolymer composition after purification. A control experiment (**LP2**) was then performed under identical conditions to **LP3** without the presence of the RAFT chain transfer agent in order to probe the effect of CPDT. **LP2** (OEGMA-*c*-MDO) was obtained after 16 h with a PDI of 13.59, indicating that CPDT is able to control the polymerization to a reasonable extent. Poly($OEGMA_{300}$) is known to have an lower critical solution temperature (LCST) of 64 °C, the incorporation of MDO drastically reduces this phase transition temperature, we observed that **LP3** and **LP4** possess LCSTs of 35 °C and 42 °C, respectively (ESI, Fig. S9). These three experiments confirm that the co-polymerization of MDO and OEGMA proceeds with improved PDI in the presence of CPDT, reducing the amount of MDO relative

to OEGMA further improves the resulting PDI, and that increasing the amount of MDO relative to OEGMA reduces the LCST phase transition temperature. **LP5** (DEAEMA-*c*-MDO) was prepared with a DEAEMA: MDO: CPDT: AIBN molar ratio of 100: 100: 1: 0.5, at 70 °C for 16 h. This experiment proceeded with a similar PDI (2.31) to **LP4**, again we observe a copolymer composition via ^{1}H NMR spectroscopy (ESI, Fig. S10) similar to monomer conversion. Hydrolysis of each polymer (**LP2-5**) was carried out under accelerated alkali conditions with $NaOH_{(aq)}$. Size exclusion chromatography displayed the hydrolysis of each polymer into short oligomers (ESI, Fig. S11), confirming the incorporation of ester functionalities within the polymer main-chain.

Table 3. Synthesis and characterization of main-chain degradable linear (**LP2-6**), diblock (**DB2**), hyperbranched (**HB5-8**) and star hyperbranched (**SHB5-8**) polymers.

ID	RAFT CTA [eq.]	Monomer [eq.]	CKA [eq.]	Cross-Linker [eq.]	Initiator [eq.]	Time (h)	Temp (°C)	Monomer Conv.[a] (%)	MDO Conv.[a] (%)	M_n[b] (g mol^{-1})	M_w[b] (g mol^{-1})	PDI[b] (M_w/M_n)	Hydrolysis M_n[b] (g mol^{-1})
LP2	-	OEGMA [100]	MDO [150]	-	AIBN [0.5]	16	70	99	30	17,400	236,500	13.59	900
LP3	CPDT [1]	OEGMA [100]	MDO [150]	-	AIBN [0.5]	16	70	95	25	14,300	63,600	4.45	1,200
LP4	CPDT [1]	OEGMA [100]	MDO [100]	-	AIBN [0.5]	16	70	94	25	15,000	36,100	2.41	2,000
LP5	CPDT [1]	DEAEMA [100]	MDO [100]	-	AIBN [0.5]	16	70	90	27	8,400	19,400	2.31	1,100
LP6	CPDT [1]	DEAEMA [100]	MDO [100]	-	AIBN [0.5]	8	70	50	15	3,600	7,900	2.19	1,200
DB2	**LP6** [1]	OEGMA [80]	MDO [120]	-	AIBN [0.5]	16	70	96	27	11,000	48,400	4.40	1,500
HB5	CPDT [1]	DEAEMA [100]	MDO [100]	DEGDMA [2]	AIBN [0.5]	8	70	50	17	1,700	5,100	3.00	1,300
HB6	CPDT [1]	DEAEMA [100]	MDO [100]	DEGDMA [2]	AIBN [0.5]	8	90	71	20	1,800	5,900	3.28	1,200
HB7	CPDT [1]	DEAEMA [100]	MDO [100]	DEGDMA [2]	ACHN [0.5]	5	100	92	32	3,000	8,700	2.90	1,200
HB8	CPDT [1]	DEAEMA [50]	MDO [50]	DEGDMA [2]	ACHN [0.5]	5	100	91	30	4,400	13,500	3.01	1,400
SHB5	**HB5** [1]	OEGMA [80]	MDO [120]	-	AIBN [0.5]	16	70	98	28	5,900	26,000	4.41	1,500
SHB6	**HB6** [1]	OEGMA [80]	MDO [120]	-	AIBN [0.5]	16	70	99	27	7,600	29,000	3.82	1,500
SHB7	**HB7** [1]	OEGMA [80]	MDO [120]	-	AIBN [0.5]	16	70	99	30	6,500	31,000	4.77	1,400
SHB8	**HB8** [1]	OEGMA [80]	MDO [120]	-	AIBN [0.5]	16	70	99	33	7,200	34,600	4.81	1,600

All reactions were performed with 7.5 mmol MDO in 50 wt % DMF (wrt combined monomer mass). [a] Determined by ^{1}H NMR spectroscopy, [b] determined by SEC (in THF) against PS standards. AIBN = azobisisobutyronitrile and ACHN = azobis(cyanocyclohexane).

Attempts to chain-extend **LP3** and **LP4** with DEAEMA and MDO were unsuccessful, as was an attempt to chain-extend **LP5** with OEGMA and MDO. Each unsuccessful experiment resulted in the presence of the original macro-RAFT CTA precursor and an additional uncontrolled polymer of very high PDI (> 12). The increased molar equivalence of AIBN employed could negatively influence chain-extension efficiency. Unfortunately this radical concentration, relative to RAFT chain transfer agent, is required to incorporate around 20 mol. % MDO within the methacrylate-based copolymer. **LP6** (DEAEMA-*c*-MDO) was then prepared under similar conditions to **LP5**, but with a shorter reaction time, our hypothesis being that extended reaction time leads to the loss of RAFT-group functionality. This resulted in a lower conversion (50 %), however **LP6** was successfully chain-extended with OEGMA and MDO, affording **DB2**. An OEGMA: MDO ration of 1: 1.5 was selected for the chain-extension, from the previous experiments we knew this would slightly raise the PDI, but we wanted to target a lower LCST which would make thermoresponsive self-assembly easier to investigate. ^{1}H NMR spectroscopy (ESI, Fig. S12) of **DB2** confirmed a ratio of DEAEMA to OEGMA which was consistent with the monomer conversions obtained for each stage. After chain-extension we observe an increase in PDI from 2.19 to 4.40. SEC analysis (Fig. 6(a)) confirmed a successful chain-extension of **LP6** to **DB2**, and we also confirmed that **DB2** undergoes ester hydrolysis to short oligomers. This result was very promising as we were able to retain RAFT-group functionality and therefore the living nature of the polymer, and the incorporation of MDO was achieved during each polymerization step.

The next challenge was to prepare star hyperbranched polymer architectures with main-chain degradability throughout the structure. This would be more challenging as the formation of hyperbranched polymers requires high conversion to complete interchain cross-linking. For the degradable hyperbranched polymers (**HB5-8**) the ratio of RAFT CTA to DEGDMA was kept at 1: 2, as it was for **HB1-4**. Initially, **HB5** was prepared under identical conditions to **LP6**, with the addition of the divinyl cross-linker DEGDMA. While this low methacrylate conversion (50 %) would not yield an ideal hyperbranched polymer, we wanted to confirm that the presence of DEGDMA would not prevent subsequent chain-extension. The chain-extension of **HB5** (with an OEGMA: MDO ratio of 1: 1.5) to **SHB5** was confirmed by SEC (ESI, Fig. S13(a)) as was the hydrolysis of **SHB5**. This successful chain-extension was promising but the challenge of high conversion within a shorter reaction time remained. **HB6** was prepared with AIBN at an elevated temperature of 90 °C, and a methacrylate conversion of 71 % was obtained after 8 h. **HB6** was successfully chain-extended to **SHB6** (ESI, Fig. S13(b)), confirming that increased temperature does not influence RAFT-group retention. However, a conversion of 71 % for hyperbranched polymer formation is not optimal so we decided to switch radical source to ACHN as the half-life temperature is higher compared to AIBN. **HB7** was prepared with ACHN at 100 °C and a methacrylate conversion of 92 % was obtained after 5 h. The hyperbranched polymer **HB7** (a degradable analogue of **HB3**) was chain-extended to the star hyperbranched polymer **SHB7** (a degradable analogue of **SHB3**), the successful chain-extension was confirmed by SEC Figure 6 (Fig. 6(b)),

again the incorporation of MDO was confirmed through the hydrolysis of **HB7** and **SHB7**. Finally, **HB8** was prepared with ACHN at 100 °C for 5 h, with a ratio of CPDT: DEAEMA: MDO: DEGDMA: ACHN of 1: 50: 50: 2: 0.5. Resulting in a degradable analogue of **HB2**, the lower ratio of DEAEMA and MDO relative to CPDT, DEGDMA and ACHN (in comparison to **HB7**) meant that the ether protons of DEGDMA (δ 3.65 ppm) could clearly be observed by ^{1}H NMR spectroscopy (Fig. 5(a)) confirming successful hyperbranched polymer formation. **HB8** was chain-extended to **SHB8**, confirmed by SEC (ESI, Fig. S14(a)) and ^{1}H NMR spectroscopy (Fig. 5(b)). The monomer compositions of **HB5-8** and **SHB5-8** obtained from ^{1}H NMR spectroscopy were consistent with the monomer conversions obtained after polymerization. The synthesis of **HB5-8** all proceeded with slightly higher PDIs (2.9 – 3.3) when compared to **LP4-6** (2.2 – 2.4), this is a result of cross-linking and is consistent with the formation of hyperbranched polymers and our previous observations comparing **LP1** to **HB1-4** (Table 1). The chain-extension of **HB5-8** to the corresponding **SH5-8** proceeds with an increase in PDI due to the ratio of methacrylate to CKA increasing from 1: 1 to 1: 5 during the chain-extension. These experiments confirm that reaction time, initiator and temperature have to be carefully considered in order to obtain high methacrylate conversions with the ability to chain-extended in the presence of the cyclic ketene acetal MDO.

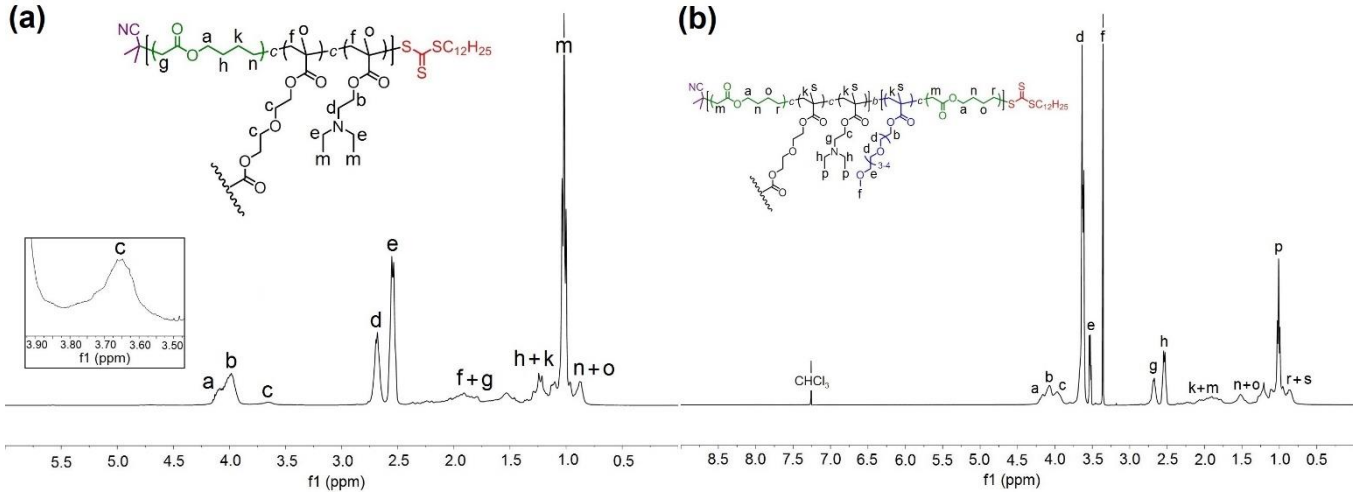

Fig 5. ^{1}H NMR ($CDCl_3$) spectra of (a) main-chain degradable hyperbranched polymer **HB8** and (b) chain-extended star hyperbranched polymer **SHB8**.

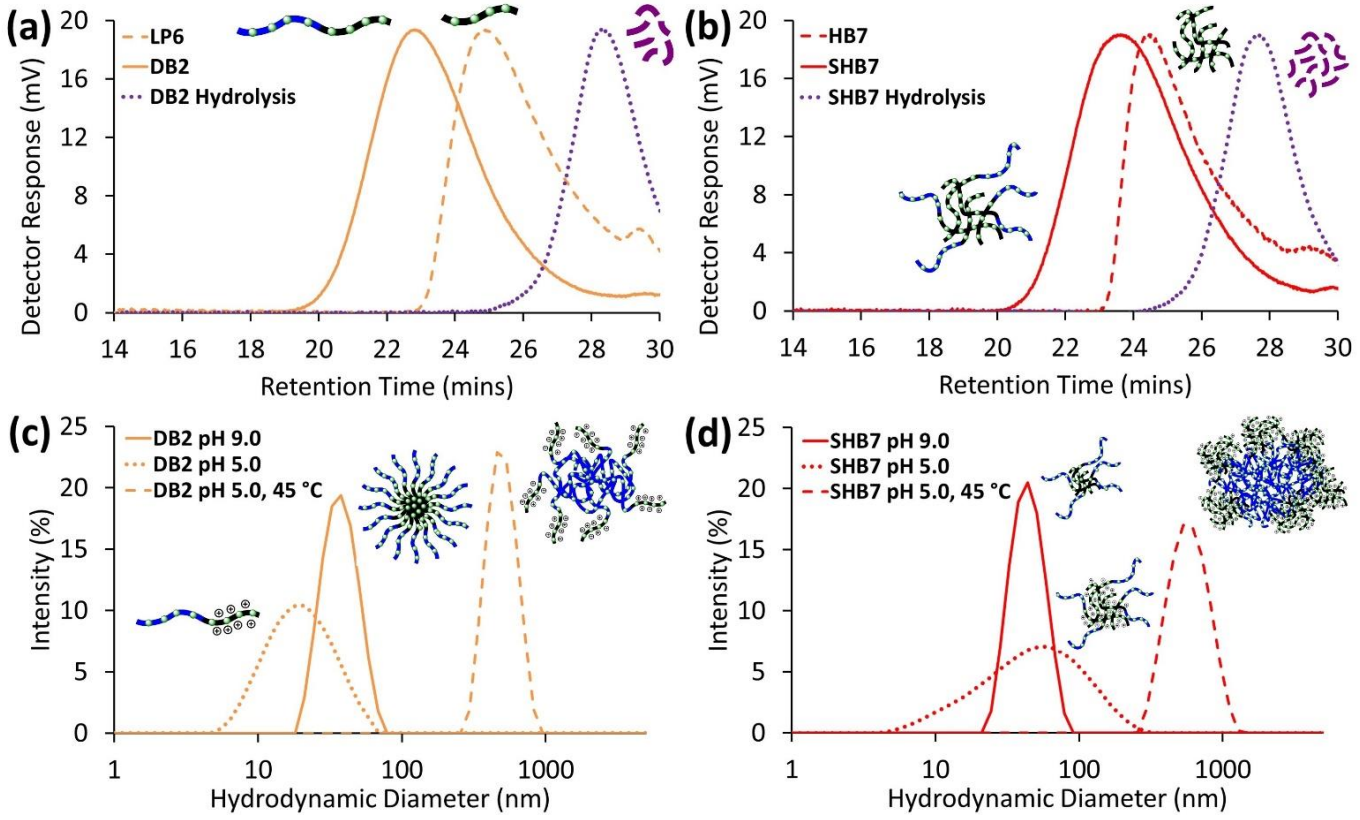

Fig. 6 SEC refractive index traces (in THF) of (a) linear polymer **LP6** (dashed line) followed by chain-extension to **DB2** (solid line) and subsequent hydrolysis of **DB2** (dotted line) and (b) hyperbranched polymer **HB7** (dashed line) followed by chain-extension to **SHB7** (solid line) and subsequent hydrolysis of **SHB7** (dotted line). DLS analysis in H_2O (3 mg/mL) of (c) diblock copolymer **DB2** and (d) star hyperbranched polymer **SHB7** at pH 5.0 (dotted lines) and pH 9.0 (solid lines) and pH 5.0 at 45 °C (dashed lines).

The pH- and thermoresponsive behavior of the degradable diblock (**DB2**) and degradable star hyperbranched polymers (**SHB7-8**) was then investigated. The incorporation of MDO into the OEGMA block significantly lowers the LCST from 64 °C to approx. 40 °C which is more appealing experimentally and for potential application. The main-chain degradable diblock polymer **DB2** displayed interesting 'schizophrenic' self-assembly behavior (Fig. 6(c)). At pH 5.0 the polymer was fully soluble and displayed a D_h = 20 nm (PDI = 0.205), micellization occurs upon increasing the pH to 9.0, displaying a D_h = 42 nm (PDI = 0.047). These result are very similar to **DB1** (ESI, Fig. S4(b) and Table 2). At pH 5.0 and a temperature of 45 °C we observed self-assembly into large aggregates of D_h = 520 nm (PDI = 0.104). This large size is presumable due to the ratio of protonated (hydrophilic) DEAEMA block to the collapsed (hydrophobic) OEGMA block upon temperature induced phase transition. At pH 9.0 and a temperature of 45 °C the polymer completely precipitates from solution. The responsive behavior of **SHB7** was perhaps even more interesting (Fig. 6(d)). At pH 5.0 the star hyperbranched polymer was fully soluble and displayed a D_h = 61 nm (PDI = 0.399). However, upon increasing the pH to 9.0 we did not observed self-assembly into larger star hyperbranched polymer micelles as observed with **SHB1-4**, instead we observe a size reduction to D_h = 45 nm (PDI = 0.041). Upon tertiary amine deprotonation the hyperbranched polymer core collapses and is kept in solution by the linear OEGMA-*c*-MDO corona without aggregation into star hyperbranched polymer micelles. This observation is counterintuitive as the corona of **SHB7** is less hydrophilic when compared to **SHB1-4**. It would be reasonable to predict that the incorporation of MDO within the corona would lower its hydrophilicity and would result in a greater need for star hyperbranched polymer self-assembly. Our current hypothesis is that the incorporation of hydrophobic MDO monomer units could force the OEGMA units to orientate their short PEG chains towards the nanoparticle exterior, in order to remain in solution even at low pH. This driving force could result in a very PEGylated surface, but would also reduce conformational freedom and inhibit self-assembly. This driving force might not exist with **SHB1-4** with their hydrophilic coronas possessing more conformational freedom due to increased hydrophilicity. At pH 5.0 and a temperature of 45 °C we observed the self-assembly of **SHB7** into large aggregates of D_h = 600 nm (PDI = 0.142), and at pH 9.0 and a temperature of 45 °C **SHB7** completely precipitates from solution. **SHB8** displayed a similar pH- and thermoresponsive profile (ESI, Fig. S14(b)) to **SHB7**. At pH 5.0 **SHB8** is fully soluble and displays a D_h = 91 nm (PDI = 0.323), at pH 9.0 the star hyperbranched polymer reduces in size to D_h = 58 nm (PDI = 0.135), at pH 5.0 and a temperature of 45 °C self-assembly into larger aggregates occurs with a D_h = 815 nm (PDI = 0.168). While **DB2** behaved as expect, we see thought-provoking differences in the pH-responsiveness behavior between **SHB1-4** and **SHB7-8**. These curious results suggest that the effect of MDO incorporation on stimuliresponsive behavior and subsequent self-assembly is a very interesting topic, which is currently under further investigation.

Conclusions

RAFT polymerization has been used to prepare a series of star hyperbranched (**SHB1-4**) polymers which are comprised of a DEAEMA-based covalently cross-linked hyperbranched core and an OEGMA-based linear corona. These materials undergo pH-triggered self-assembly and after optimizing the synthetic parameters (**SHB2**) a corresponding linear diblock (**DB1**) polymer was prepared. We then investigated the uptake and release of Indomethacin within the interior of the SHB and DB polymeric structures, the SHB polymer which can be described as unimolecular micelles showed significantly improve uptake and a slower release profile when compared to the conventional diblock polymer micelle. To further demonstrate the utility of the SHB polymer morphology we performed aminolysis of the RAFT trithiocarbonate z-group located at the SHB periphery to reactive thiol functionalities which then facilitated post-polymerization functionalized via thiol-ene click chemistry and hydrogel formation via disulfide formation under oxidative conditions. We believe that SHB polymers are very attractive alternatives to conventional diblock polymer micelles which are prone to rapid release of hydrophobic actives and undesirable disassembly under dilute conditions. To further improve their application potential the incorporation of a cyclic ketene acetal monomer into each bock was achieved (**DB2** and **SHB5-8**), imparting main-chain polyester degradability. The ability to precisely control the synthesis of SHB polymers is feasible with the RAFT polymerization technique and can lead to very useful polymeric materials which are synthetically straightforward, easily tunable, stimuliresponsive and biodegradable. We feel that the combination of reversible-deactivation radical polymerization techniques with cyclic ketene acetal radical ring-opening chemistry can result in very interesting polymeric architectures. Understanding how to incorporate CKAs within vinyl-based multi-block copolymers is a very useful tool which can furnish polymeric materials with both main-chain degradability and stimuliresponsive self-assembly behavior.

Conflicts of Interest

There are no conflicts to declare

Acknowledgments

The joint PhD studentship between the University of Liverpool and the A*Star Research Attachment Program (ARAP) scholarship is gratefully thanked for support of this research. The Agency for Science, Technology and Research (A*STAR), Science and Engineering Research Council, Specialty Chemicals AME IAF-PP Programme Grant A1786a0025 is also thanked for financial support.

References

1. G. Moad, E. Rizzardo and S. H. Thang, *Aust. J. Chem.*, 2005, **58**, 379-410.
2. C. J. Hawker, A. W. Bosman and E. Harth, *Chem. Rev.*, 2001, **101**, 3661-3688.
3. K. Matyjaszewski and J. H. Xia, *Chem. Rev.*, 2001, **101**, 2921-2990.
4. W. A. Braunecker and K. Matyjaszewski, *Prog. Polym. Sci.*, 2007, **32**, 93-146.

5. C. Boyer, M. H. Stenzel and T. P. Davis, *J. Polym. Sci., Part A*, 2011, **49**, 551-595.
6. A. Gregory and M. H. Stenzel, *Prog. Polym. Sci.*, 2012, **37**, 38-105.
7. R. M. England and S. Rimmer, *Polym. Chem.*, 2010, **1**, 1533-1544.
8. G. Riess, *Prog. Polym. Sci.*, 2003, **28**, 1107-1170.
9. D. E. Discher and A. Eisenberg, *Science*, 2002, **297**, 967-973.
10. C. Gao and D. Yan, *Prog. Polym. Sci.*, 2004, **29**, 183-275.
11. B. Voit, *J. Polym. Sci. Pol. Chem.*, 2000, **38**, 2505-2525.
12. K. Inoue, *Prog. Polym. Sci.*, 2000, **25**, 453-571.
13. M. Jikei and M. Kakimoto, *Prog. Polym. Sci.*, 2001, **26**, 1233-1285.
14. B. Helms, S. J. Guillaudeu, Y. Xie, M. McMurdo, C. J. Hawker and J. M. J. Frechet, *Angew. Chem., Int. Ed.*, 2005, **44**, 6384-6387.
15. Y. Shen, M. Kuang, Z. Shen, J. Nieberle, H. W. Duan and H. Frey, *Angew. Chem.-Int. Edit.*, 2008, **47**, 2227-2230.
16. Q. Zhu, F. Qiu, B. S. Zhu and X. Y. Zhu, *RSC Adv.*, 2013, **3**, 2071-2083.
17. K. Uhrich, *Trends Polym. Sci.*, 1997, **5**, 388-393.
18. A. Star and J. F. Stoddart, *Macromolecules*, 2002, **35**, 7516-7520.
19. M. Bednarek, T. Biedron, J. Helinski, K. Kaluzynski, P. Kubisa and S. Penczek, *Macromolecular Rapid Communications*, 1999, **20**, 369-372.
20. H. Magnusson, E. Malmstrom and A. Hult, *Macromolecular Rapid Communications*, 1999, **20**, 453-457.
21. H. Chen and J. Kong, *Polym. Chem.*, 2016, **7**, 3643-3663.
22. J. M. J. Frechet and C. J. Hawker, *Reactive & Functional Polymers*, 1995, **26**, 127-136.
23. J. M. J. Frechet, M. Henmi, I. Gitsov, S. Aoshima, M. R. Leduc and R. B. Grubbs, *Science*, 1995, **269**, 1080-1083.
24. C. J. Hawker, J. M. J. Frechet, R. B. Grubbs and J. Dao, *J. Am. Chem. Soc.*, 1995, **117**, 10763-10764.
25. A. P. Vogt, S. R. Gondi and B. S. Sumerlin, *Aust. J. Chem.*, 2007, **60**, 396-399.
26. H. Sun, C. P. Kabb and B. S. Sumerlin, *Chemical Science*, 2014, **5**, 4646-4655.
27. K. Matyjaszewski, S. G. Gaynor and A. H. E. Muller, *Macromolecules*, 1997, **30**, 7034-7041.
28. Y. F. Tao, J. P. He, Z. M. Wang, J. Y. Pan, H. J. Jiang, S. M. Chen and Y. L. Yang, *Macromolecules*, 2001, **34**, 4742-4748.
29. H. F. Gao and K. Matyjaszewski, *Prog. Polym. Sci.*, 2009, **34**, 317-350.
30. B. L. Liu, A. Kazlauciunas, J. T. Guthrie and S. Perrier, *Macromolecules*, 2005, **38**, 2131-2136.
31. B. L. Liu, A. Kazlauciunas, J. T. Guthrie and S. Perrier, *Polymer*, 2005, **46**, 6293-6299.
32. N. R. B. Boase, I. Blakey, B. E. Rolfe, K. Mardon and K. J. Thurecht, *Polym. Chem.*, 2014, **5**, 4450-4458.
33. K. W. Wang, H. Peng, K. J. Thurecht, S. Puttick and A. K. Whittaker, *Polym. Chem.*, 2016, **7**, 1059-1069.
34. S. Pal, M. R. Hill and B. S. Sumerlin, *Polym. Chem.*, 2015, **6**, 7871-7880.
35. P. R. Bachler, K. E. Forry, C. A. Sparks, M. D. Schulz, K. B. Wagener and B. S. Sumerlin, *Polym. Chem.*, 2016, **7**, 4155-4159.
36. A. Tardy, J. Nicolas, D. Gigmes, C. Lefay and Y. Guillaneuf, *Chem. Rev.*, 2017, **117**, 1319-1406.
37. W. J. Bailey, Z. Ni and S. R. Wu, *J. Polym. Sci. Polym. Chem. Ed.*, 1982, **20**, 3021-3030.
38. A. Tardy, J. C. Honore, D. Siri, D. Gigmes, C. Lefay and Y. Guillaneuf, *Polym. Chem.*, 2017, **8**, 5139-5147.
39. S. Agarwal, *Polym. Chem.*, 2010, **1**, 953-964.
40. C. G. Decker and H. D. Maynard, *Eur. Polym. J.*, 2015, **65**, 305-312.
41. G. G. Hedir, M. C. Arno, M. Langlais, J. T. Husband, R. K. O'Reilly and A. P. Dove, *Angew. Chem.-Int. Edit.*, 2017, **56**, 9178-9182.
42. M. R. Hill, E. Guegain, J. Tran, C. A. Figg, A. C. Turner, J. Nicolas and B. S. Sumerlin, *ACS Macro Lett.*, 2017, **6**, 1071-1077.
43. T. He, Y. F. Zou and C. Y. Pan, *Polym. J.*, 2002, **34**, 138-143.
44. C. A. Bell, G. G. Hedir, R. K. O'Reilly and A. P. Dove, *Polym. Chem.*, 2015, **6**, 7447-7454.
45. J. F. Lutz, J. Andrieu, S. Uzgun, C. Rudolph and S. Agarwal, *Macromolecules*, 2007, **40**, 8540-8543.
46. I. S. Chung and K. Matyjaszewski, *Macromolecules*, 2003, **36**, 2995-2998.
47. J. Y. Yuan and C. Y. Pan, *Eur. Polym. J.*, 2002, **38**, 2069-2076.
48. A. Tardy, V. Delplace, D. Siri, C. Lefay, S. Harrisson, B. D. A. Pereira, L. Charles, D. Gigmes, J. Nicolas and Y. Guillaneuf, *Polym. Chem.*, 2013, **4**, 4776-4787.
49. V. Delplace, E. Guegain, S. Harrisson, D. Gigmes, Y. Guillaneuf and J. Nicolas, *Chemical Communications*, 2015, **51**, 12847-12850.
50. E. Guegain, J. P. Michel, T. Boissenot and J. Nicolase, *Macromolecules*, 2018, **51**, 724-736.
51. J. Y. Yuan and C. Y. Pan, *Eur. Polym. J.*, 2002, **38**, 1565-1571.
52. V. Delplace, A. Tardy, S. Harrisson, S. Mura, D. Gigmes, Y. Guillaneuf and J. Nicolas, *Biomacromolecules*, 2013, **14**, 3769-3779.
53. G. G. Hedir, C. A. Bell, N. S. Ieong, E. Chapman, I. R. Collins, R. K. O'Reilly and A. P. Dove, *Macromolecules*, 2014, **47**, 2847-2852.
54. G. G. Hedir, A. Pitto-Barry, A. P. Dove and R. K. O'Reilly, *J. Polym. Sci. Pol. Chem.*, 2015, **53**, 2699-2710.
55. G. G. Hedir, C. A. Bell, R. K. O'Reilly and A. P. Dove, *Biomacromolecules*, 2015, **16**, 2049-2058.
56. G. Turturica, M. Andrei, P. O. Stanescu, C. Draghici, D. M. Vuluga, A. Zaharia, A. Sarbu and M. Teodorescu, *Colloid Polym. Sci.*, 2016, **294**, 743-753.
57. M. Andrei, P. O. Stanescu, C. Draghici and M. Teodorescu, *Colloid Polym. Sci.*, 2017, **295**, 1805-1816.
58. Y. Wei, E. J. Connors, X. R. Jia and C. Wang, *J. Polym. Sci. Pol. Chem.*, 1998, **36**, 761-771.
59. C. J. Hawker, R. Lee and J. M. J. Frechet, *J. Am. Chem. Soc.*, 1991, **113**, 4583-4588.
60. S. Maji, F. Mitschang, L. N. Chen, Q. Jin, Y. X. Wang and S. Agarwal, *Macromol. Chem. Phys.*, 2012, **213**, 1643-1654.
61. Q. Jin, S. Maji and S. Agarwal, *Polym. Chem.*, 2012, **3**, 2785-2793.
62. G. E. Roberts, M. L. Cootes, J. P. A. Heuts, L. M. Morris and T. P. Davis, *Macromoelcules*, 1999, **32**, 1332-1340.
63. L. Q. Ren, C. Speyerer and S. Agarwal, *Macromolecules*, 2007, **40**, 7834-7841.

Graphical Abstract

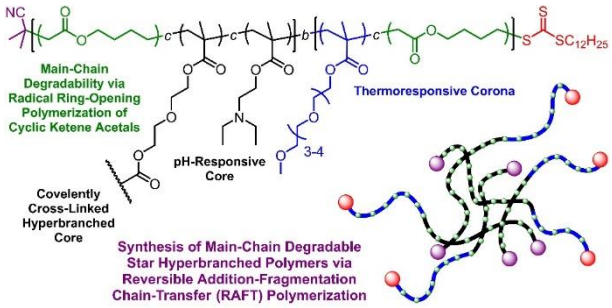

Dual stimuliresponsive main-chain degradable star hyperbranched polymers have been synthesized via cyclic ketene acetal radical ring-opening and RAFT-based methacrylate copolymerization